

Localization of Third Sound by a Disordered Substrate

Scott M. Cohen and Jonathan Machta

Laboratory for Low Temperature Physics, Department of Physics and Astronomy, University of Massachusetts, Amherst, Massachusetts 01003

(Received 13 February 1985)

We propose the use of third sound in ^4He films on a disordered substrate as a system for the study of Anderson localization in two dimensions. Quantitative predictions for the localization length are made with use of the self-consistent diagrammatic theory of localization. Dramatic effects are predicted in an experimentally accessible regime.

PACS numbers: 67.40.Pm, 67.40.Rp, 71.55.Jv

Anderson localization is a general feature of wave propagation in disordered media. Though most theoretical and experimental effort has been devoted to understanding localization in solid-state systems,¹ several authors have pointed out that localization may be observable in a variety of other systems.²⁻⁵ The purpose of this Letter is to argue that the third-sound modes of a ^4He film on a disordered substrate will exhibit Anderson localization. Using the self-consistent diagrammatic theory of localization^{1,6} applied to the classical wave equation,⁷ we give quantitative results for the localization length and predict dramatic effects in an experimentally accessible regime.

The propagation of third sound on disordered substrates has recently been studied in several laboratories.^{8,9} We shall focus attention on the experiments of Smith *et al.*⁸ In these studies the substrate is a flat glass slide to which disorder is introduced by dusting with small (1–10 μm) particles at densities of the order of 10^5 cm^{-2} . Third-sound pulses are generated at one end of the slide and detected at one or more locations away from the source. The shape and time of arrival of the pulse is monitored and compared to identical pulses propagated on a clean substrate.

Figure 1 shows a cross section of a single dust particle and the film profile surrounding it. The film is bound to the substrate and the dust particle by the van der Waals force, and the profile near the dust particle is determined by the competition between the van der Waals attraction and surface tension. The equilibrium profile may be obtained by minimization of the grand

potential, with the temperature and chemical potential held fixed. For our purposes, the important feature of this profile is the relatively large volume of fluid collected around the base of the dust particle. We denote the extra volume of fluid associated with a single dust particle by ΔV .

The mechanism by which the dust particles serve to scatter third sound is as follows: The characteristic times and distances associated with these scatterers are much shorter than those associated with the sound modes, so that the film profile around a scatterer at \mathbf{r}_0 remains in local equilibrium with the surrounding film and is determined by the local chemical potential $\mu(\mathbf{r}_0, t)$, or equivalently, the local height $h(\mathbf{r}_0, t)$. As a sound wave passes, ΔV maintains its local equilibrium value, $\Delta V(h(\mathbf{r}_0, t))$. Thus, by continuity, an extra amount of fluid, proportional to $\alpha \equiv d\Delta V/dh$, flows into and out of the region near the scatterer during the disturbance. For long wavelengths and low frequencies, we show that α is the only quantity needed to characterize a scatterer.

The Lagrangian density per unit area is given by

$$\begin{aligned} \mathcal{L}(\mathbf{r}, t) \\ = \frac{1}{2} m \sigma_0 [\nabla \phi(\mathbf{r}, t)]^2 + \Omega(\dot{\phi}(\mathbf{r}, t)/m - \mu_0; \mathbf{r}), \end{aligned} \quad (1)$$

where m is the atomic mass, μ_0 is the equilibrium chemical potential, σ_0 is the number of atoms per unit area on a clean substrate with chemical potential μ_0 , ∇ is the gradient parallel to the substrate, and $\Omega(\mu; \mathbf{r})$ is the grand potential per unit area as a function of the chemical potential and position. At fixed temperature and surface area,

$$d\Omega(\mu; \mathbf{r}) = -\sigma(\mu; \mathbf{r}) d\mu, \quad (2)$$

where $\sigma(\mu; \mathbf{r})$ is the number of fluid particles per unit area. Both Ω and σ are coarse grained over cells which, on average, contain many scatterers. At low temperatures, the thermal component of third sound is small and we ignore the dependence of Ω on the temperature. The field variable, $\phi(\mathbf{r}, t)$, is defined via the local chemical potential according to

$$\dot{\phi}(\mathbf{r}, t) = -m^{-1}[\mu(\mathbf{r}, t) - \mu_0]. \quad (3)$$

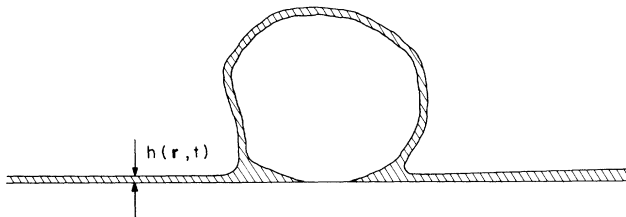


FIG. 1. Cross section of a single scatterer and the film profile surrounding it, showing capillary condensation around the base of the scatterer.

The force law for the superfluid on a flat substrate is $m\dot{\mathbf{v}}(\mathbf{r},t) = -\nabla\mu(\mathbf{r},t)$, so that far from any scatterer, $\phi(\mathbf{r},t)$ corresponds to the velocity potential.

Using the Euler-Lagrange equations and the thermodynamic relation, Eq. (2), we obtain the following wave equation for the fluid;

$$m \frac{\partial \sigma}{\partial \mu} \frac{\partial^2 \phi}{\partial t^2} - \sigma_0 \nabla^2 \phi = 0. \quad (4)$$

Since, as discussed above, the areal density of the fluid is modified by the scatterers, the derivative, $\partial\sigma/\partial\mu$, depends on the areal density of scatterers, $\rho(\mathbf{r})$, and we obtain a wave equation with a spatially varying sound speed,

$$\left[\frac{1}{c_0^2} [1 + \rho(\mathbf{r})\alpha] \frac{\partial^2}{\partial t^2} - \nabla^2 \right] \phi(\mathbf{r},t) = 0, \quad (5)$$

where c_0 is the speed of third sound on a clean substrate, $c_0 = [(h/m)\partial\mu/\partial h]^{1/2}$.

In Eq. (1), contributions to the kinetic energy due to the scatterers have been omitted. These contributions depend on the geometric area of the scatterer rather than the effective area, α . For the scatterers under discussion, and thick (10–30 atomic layers) films, α is much larger than the geometric area so that kinetic-energy contributions can be ignored. For hard disks, on the other hand, $-\alpha$ is equal to the geometric area of the scatterer and the kinetic-energy term in the Lagrangian density is significantly modified. This accounts for the difference between our results and those obtained by Kirkpatrick⁷ for hard disks. In deriving Eq. (5) we have also ignored dissipation which should be a good approximation for sufficiently

low temperatures.^{10,11}

The scatterers are Poisson distributed on the substrate, so that for long wavelengths, $\rho(\mathbf{r})$ can be approximated by a delta-correlated Gaussian random variable. The average value, ρ_0 , of $\rho(\mathbf{r})$ can be included in a renormalized sound speed, \bar{c} , leading to the following disordered wave equation,

$$\left[\frac{1}{\bar{c}^2} [1 + \chi(\mathbf{r})] \frac{\partial^2}{\partial t^2} - \nabla^2 \right] \phi(\mathbf{r},t) = 0, \quad (6)$$

where

$$\bar{c} = c_0(1 + \rho_0\alpha)^{-1/2}, \quad (7)$$

and $\chi(\mathbf{r}) = \alpha[\rho(\mathbf{r}) - \rho_0](1 + \alpha\rho_0)^{-1}$ is a Gaussian variable with zero mean,

$$\langle \chi(\mathbf{r}) \rangle = 0, \quad (8a)$$

and variance given by

$$\langle \chi(\mathbf{r})\chi(\mathbf{r}') \rangle = \gamma^2 \sigma(\mathbf{r} - \mathbf{r}') \quad (8b)$$

with

$$\gamma^2 = \rho_0^{1/2} \alpha (1 + \rho_0\alpha)^{-1/2}. \quad (8c)$$

Properties of the model can be obtained from a perturbation expansion in powers of γ^2 using standard many-body techniques. We shall consider the average Green's function and the average squared Green's function. For each realization of the disorder, the Green's function, $G(rt|r't')$ satisfies the wave equation (6) with a delta-function source term. Taking the Fourier transform of the average of the Green's function and expanding the self-energy, $\Sigma_E(k)$, to order γ^2 , we obtain

$$G_E(\mathbf{k}) \equiv \int_0^\infty dt \int d^2(r-r') e^{i\mathbf{k}\cdot(\mathbf{r}-\mathbf{r}') - i(E+i\epsilon)t} \langle G(\mathbf{r}t|\mathbf{r}'0) \rangle = [(E/\bar{c})^2 - k^2 - \Sigma_E(\mathbf{k})]^{-1}, \quad (9)$$

with

$$\Sigma_E(\mathbf{k}) = i\gamma^2 E^4 / 4\bar{c}^4 + O(\gamma^4). \quad (10)$$

For sufficiently low frequency, the self-energy is small and the dominant effect of the disorder is to diminish the propagation speed by an amount given by Eq. (7). At somewhat higher frequencies, there will be attenuation of the wave due to multiple scattering, with an attenuation length given by

$$l(E) = 8\bar{c}^3 / \gamma^2 E^3. \quad (11)$$

Both of these effects have been verified qualitatively in experiments of the kind described above.^{8,12}

When the average Green's function predicts strong attenuation of a signal it no longer correctly describes propagation on a single disordered substrate. The Green's function, $G(rt|r't')$ fluctuates from one realization to another and may take both positive and negative values, so that for strong disorder, its average is much smaller in magnitude than a typical value. We therefore study the average of the square of the Green's function.¹ The Fourier transform of the square of the Green's function introduces a frequency convolution having a kernel, $P_E(\mathbf{k}, \omega)$, which we call the intensity propagator:

$$P_E(\mathbf{k}, \omega) = \int d^2(r-r') e^{-i\mathbf{k}\cdot(\mathbf{r}-\mathbf{r}')} \langle G_{E+\omega/2}^+(\mathbf{r}|\mathbf{r}') G_{E-\omega/2}^-(\mathbf{r}|\mathbf{r}') \rangle, \quad (12)$$

where $-$ and $+$ refer to advanced and retarded Green's functions, respectively. If the system is excited by a pulse

at the origin of width $\Delta E \gg \omega$ then $P_E(\mathbf{k}, \omega)$ is the \mathbf{k} and ω Fourier component of the average intensity resulting from the E Fourier component of the pulse.

The intensity propagator can be expanded in terms of $G_E(\mathbf{k}, \omega)$, and averaged over pairs of scattering events which correlate the two Green's functions in Eq. (12). This expansion is diagrammatically identical to that arising in the self-consistent many-body theory of electron localization.⁶ The calculation as a whole is similar to the hard-disk calculation of Ref. 7, differing primarily in the angular dependence of the vertex. Details of the calculation will be presented in a future paper. To order γ^2 the expansion of the intensity propagator leads to a diffusive pole, while higher-order terms yield divergent integrals. Among the most divergent diagrams are the maximally crossed diagrams first discussed by Langer and Neal.¹³ For small k and ω , these can be resummed and will contribute to the diffusive pole,

$$P_E(\mathbf{k}, \omega) \cong (\bar{c}^2/4E)[-i\omega + k^2 D_E(\omega)]^{-1}, \quad (13)$$

where the diffusion coefficient is given by

$$\frac{1}{D_E(\omega)} = \frac{1}{D_E^{(0)}} + \frac{\gamma^2 E^2}{4\pi^2 \bar{c}^2} \int_{q < l(E)^{-1}} d^2 q \frac{1}{(-i\omega + q^2 D_E^{(0)})}, \quad (14)$$

and

$$D_E^{(0)} = 2\bar{c}^4/\gamma^2 E^3 \quad (15)$$

is the diffusion coefficient obtained from the lowest-order diagram. The integral in Eq. (14) results from the sum of the maximally crossed diagrams and diverges to $-\infty$ as $\omega \rightarrow 0$. Physically, the divergence arises from coherent backscattering as in the quantum case. Following Vollhardt and Wolfle,⁶ we replace $D_E^{(0)}$ with $D_E(\omega)$ in this integral. This leads to an integral equation for $D_E(\omega)$ which, for small ω and E , yields

$$D_E(\omega) = -i\omega \xi^2(E), \quad (16)$$

where the localization length $\xi(E)$ is

$$\xi(E) = l(E) \exp(E_0/E)^2, \quad (17)$$

and the frequency E_0 is given by

$$E_0 = (2\pi)^{1/2} \bar{c}/\gamma. \quad (18)$$

The frequency dependence of the localization length given in Eq. (17) is in qualitative agreement with the field theoretic results for phonon localization obtained by John, Sompolinsky, and Stephen.¹⁴

These expressions are valid only for $E < E_0$. The meaning of Eqs. (13), (16), and (17) is that energy injected into the system at frequency E will not spread further than a characteristic distance $\xi(E)$. An alternative expression for E_0 , which may be more useful for comparison with experiment, follows from Eq. (7),

$$E_0 = (2\pi\rho_0)^{1/2} n c_0 / (n^2 - 1), \quad (19)$$

where $n = c_0/\bar{c}$ is the low-frequency index of refraction. In the experiments reported in Ref. 8, both c_0 and n vary with film thickness, with c_0 decreasing and n increasing as the film is thickened. Thus, a desirable feature of the superfluid system is that the strength of the disorder can be continuously varied by varying the film thickness. For films with $h_0 = 20$ atomic layers,

$\rho_0 \cong 10^5 \text{ cm}^{-2}$, $c_0 \cong 400 \text{ cm s}^{-1}$, and $n = 2.25$, we obtain $E_0/2\pi = 28 \text{ kHz}$, which is experimentally accessible.

In summary, we have discussed a model of wave propagation in a two-dimensional disordered medium and made quantitative predictions for the localization length of third sound in ^4He film on a rough surface. In this experimental system both the frequency and the strength of the disorder can be continuously varied through a range for which the predicted localization length goes from effectively infinite to less than a millimeter. In addition to its intrinsic interest in understanding ^4He films, this system may provide a quantitative testing ground for the basic theoretical ideas of two-dimensional localization unencumbered by complications, such as electron-electron interactions, inherent in solid-state systems.

We are pleased to acknowledge T. R. Kirkpatrick for providing us with the calculation presented in Ref. 7 prior to publication, and to R. B. Hallock and R. Guyer for extensive discussions concerning this work. This work was supported in part by the National Science Foundation under Grant No. DMR-8317442.

¹See, for instance, T. R. Kirkpatrick and J. R. Dorfman, in *Fundamental Problems in Statistical Mechanics*, edited by E. G. D. Cohen (North-Holland, Amsterdam, 1985); in *Anderson Localization*, edited by Y. Nagaoka and H. Fukuyama (Springer-Verlag, Berlin, 1982); D. J. Thouless, in *Ill-Condensed Matter*, edited by R. Balian, R. Maynard, and G. Toulouse (North-Holland, Amsterdam, 1979).

²C. H. Hodges, *J. Sound Vib.* **82**, 411 (1982).

³E. Guazzelli, E. Guyon, and B. Souillard, *J. Phys. (Paris)*, Lett. **44**, L837 (1983).

⁴D. F. Escande and B. Souillard, *Phys. Rev. Lett.* **52**, 1296 (1984).

⁵S. John, *Phys. Rev. Lett.* **53**, 2169 (1984).

⁶D. Vollhardt and P. Wolfle, Phys. Rev. Lett. **45**, 842 (1980), and Phys. Rev. B **22**, 4666 (1980).

⁷T. R. Kirkpatrick, Phys. Rev. B (to be published).

⁸D. T. Smith, M. Liebl, M. D. Bummer, and R. B. Hallock, in *Low Temperature Physics LT-17, Contributed Papers*, edited by V. Eckern *et al.* (North-Holland, Amsterdam, 1984), p. 57.

⁹M. Z. Shoushtari and K. L. Telschow, Phys. Rev. B **26**, 4917 (1982).

¹⁰B. Ratnam and J. Mochel, in *Low Temperature Physics*

LT-13, edited by K. T. Timmerhaus *et al.* (Plenum, New York, 1974), Vol. 1, p. 233.

¹¹F. M. Ellis and R. B. Hallock, Phys. Rev. B **29**, 497 (1984).

¹²J. M. Valles, D. T. Smith, and R. B. Hallock, Phys. Rev. Lett. **54**, 1528 (1985).

¹³J. S. Langer and T. Neal, Phys. Rev. Lett. **16**, 984 (1966).

¹⁴S. John, H. Sompolinsky, and M. J. Stephen, Phys. Rev. B **27**, 5592 (1983).